Published in final edited form as:
J Immunol. 2014 September 1; 193(5): 2546–2553. doi:10.4049/jimmunol.1401275.

Zfp318 regulates IgD expression by abrogating transcription termination within the *Ighm/Ighd* locus

Peter D. Pioli, **Irina Debnath**, **Janis J. Weis**, and **John H Weis***
Division of Microbiology and Immunology, Department of Pathology, University of Utah School of Medicine, Salt Lake City, Utah 84132

Abstract

The protein Zfp318 is expressed during the transition of naïve B cells from an immature to mature state. To evaluate its role in mature B cell functions, a conditional gene deficiency in *Zfp318* was created and deleted in bone marrow lineages via *Vav-Cre*. B cell development was minimally altered in the absence of the protein although transitional 2 (T2) B cell populations were depressed in the absence of Zfp318. Intriguingly, the analysis of IgM and IgD expression by maturing and mature naïve B cells demonstrated an elevated level of IgM gene products and a virtual loss of IgD products. Transcriptome analysis of Zfp318 deficient B cells revealed that only two gene products showed altered expression in the absence of Zfp318 (*Ighd* and *Sva*) demonstrating a remarkable specificity of Zfp318 action. In the absence of Zfp318, *Ighm/Ighd* transcripts, which would normally encode IgM and IgD from hnRNA transcripts via alternative splicing, lack intron and exon sequences from the IgD (*Ighd*) encoding region. This finding indicates that Zfp318, in a novel manner, functions by repressing recognition of the transcriptional termination site at the 3′ end of the terminal IgM-encoding exon allowing for the synthesis of the complete *Ighm/Ighd* hnRNA.

Introduction

The differentiation and maturation of immature transitional B cells of the marrow into mature but naïve B cells requires the coordinated expression of a number of gene products (1). Pax5 and the E2 transcriptional regulators are widely regarded as central for inducing the expression of many of the early B cell specific products (such as CD19 and IgM) in maturing marrow B cells (2, 3). Later, as B cells enter the periphery, additional transcription factors such as Mef2c, NF-κB family members, NFAT proteins, Ciita and Notch signaling family members continue the differentiation of immature B cells into mature follicular (FO) or marginal zone (MZ) cells (4, 5). A number of studies have sought to define the key transcriptional regulators and kinetics that control this pathway. In one such analysis, we examined the expression of transcriptional regulators during B cell differentiation comparing B220+ B cells obtained from the marrow of 2 week (wk) old animals (thus

#This research was funded by the Department of Pathology and the Weber Presidential Endowed Chair in Immunology. JJW was supported by NIH AI32773 and AR45521, and PDP was supported as a pre-doctoral trainee on the Hematology T32 training grant, #T-32DK007115-38.

*Address correspondence: john.weis@path.utah.edu.

lacking mature recirculating B cells), spleens from 2 wk old animals (enriched for transitional 1 and transitional 2 B cells)(T1, T2, respectively) and from B220+ B cells from mature but naïve spleens (enriched for FO and MZ B cells) (6). That gene expression screen identified a number of candidate transcriptional regulatory proteins whose expression increased with B cell maturation. Zfp318 was one such factor.

The *Zfp318* gene encodes a primary protein of 2,237 amino acids that includes domains encoding two C_2H_2 zinc fingers and a myosin II-homology sequence as well as regions rich in serine and basic amino acids (7, 8). A smaller truncated form of Zfp318 has also been described in the mouse but only the full-length form has been found as a homologue in human tissues. Zfp318 has been most extensively studied in the testes (an alternative name for the protein is Testicular Zinc-finger, TZF) where it is expressed during spermatogenesis. In transfection analyses, Zfp318 was shown to augment ligand-dependent androgen receptor (AR) control in a dose-dependent fashion (9). The possibility that Zfp318 could also play a role in B cell development via the AR was suggested by a number of studies showing B cell functions dependent upon AR (10, 11). In one such study, using a B cell specific deletion of AR, B cell development from the marrow was inhibited accompanied by enhanced autoimmune responses using a collagen-induced arthritis model (12).

To determine if Zfp318 does have a role in the development and function of B cells, we created a mouse with a conditional (Flox'd) deletion of the gene. Using *Vav-Cre* dependent deletion of the gene, we have found that B cells deficient in Zfp318 developed from marrow precursors virtually identical to that of WT. Zfp318 deficient, naïve splenic B cells did, however, demonstrate a dramatic loss of both IgD-specific transcripts and protein. IgM and IgD are synthesized from alternatively spliced transcripts positioning the same VDJ domains on either the IgM or IgD constant domains(13, 14). The gene sequences encoding the IgM transcripts have been denoted *Ighm* while those encoding IgD are identified as *Ighd*. The loss of IgD in the Zfp318 deficient B cell was due to the near exclusive use of *Ighm* transcripts to produce the IgM product due to RNA transcript termination prior to the IgD-encoding exons. The role of Zfp318 in regulating gene products is highly specific for IgD in that genome wide transcriptome analysis of B cells obtained from the Zfp318 deficient animal only identified a single additional gene with significantly altered gene expression.

As our data were being prepared for submission, a report by Enders, et al detailed the results of an ethylnitrosourea (ENU) mutagenesis screen followed by whole exome sequencing that identified a single point mutation (a non-synonymous T>C transition altering the protein sequence I1347T) within *Zfp318* that inhibited the production of IgD (15). This mutation mapped to the long form of the protein confirming its necessity versus that of the alternatively spliced, truncated form of the protein. The group also created a germline *Zfp318* null animal by gene targeting that reproduced their point mutation analyses. Those data, along with the findings presented in this report, confirm the necessity of Zfp318 for the production of IgD.

Material and Methods

Animal strains and care

Animals were housed in the Animal Resource Center (University of Utah Health Science Center, Salt Lake City, UT) according to the guidelines of the National Institute of Health for the care and use of laboratory animals. All animal protocols were reviewed and approved by the University of Utah Institutional Animal Use and Care Committee. For transcriptional profiling experiments, C57BL/6 mice were bred and maintained in house. B6.Cg-Tg(Vav1-cre)A2Kio/J mice (Stock #008449) were obtained from The Jackson Laboratories and maintained as heterozygotes. *Zfp318*$^{Fl/Fl}$ mice were bred to the *Vav-Cre* deleter strain to obtain progeny with a hematopoietic specific deletion of *Zfp318* (conditional knockout, cKO). Littermates approximating four weeks of age were used for all experiments. Animal numbers used per experiment are noted in the figure legends.

Generation of the Zfp318$^{Fl/Fl}$ animal

A targeting construct for *Zfp318* was created using a 14kb homologous fragment containing the first two exons of the gene obtained from a 129/Sv phage library. A neo targeting cassette (flanked by FRT sites) and a single LoxP site was inserted at the Hpa1 site located in the intron between exons 2 and 3. A single LoxP site was inserted at the BspE1 site 5′ of the transcription start site. 129/Sv ES clones possessing the targeted Zfp3818 gene were confirmed by Southern blot using 5′ and 3′ probes. The Neo cassette was removed by a single mating to a FRT deleter strain leaving behind the single LoxP site. Mice were bred back to C57BL/6 for 10 generations.

DNA isolation and genomic DNA PCR (gPCR)

For standard genotyping, approximately 5 mm portions of tail were boiled in 50 mM NaOH until fully dissolved. 1 M Tris was added to neutralize the NaOH. Following centrifugation to remove insoluble material, DNA was precipitated from supernatants following standard ethanol precipitation guidelines. *Vav-Cre* and *Zfp318* gPCR was performed via incorporation of [^{32}P] dCTP. Amplification products were electrophoresed in polyacrylamide sequencing gels. Products were visualized by exposure to X-ray film at −80°C. Cycling parameters are available upon request. Primer sequences are provided in Supplemental Table 1.

RNA isolation, cDNA synthesis and RT-PCR

Total RNA was isolated from cells using the Qiagen miRNeasy Mini Kit (Cat. #: 217004) according to the manufacturer's instructions. Random hexamer primers (Invitrogen, Cat. #: 58875) were used in combination with SuperScript III Reverse Transcriptase (Invitrogen, Cat. #: 56575) to synthesize cDNA. Reactions were purified using the Thermo Scientific GeneJET Purification Kit (Cat. #: K0702). Quantitative RT-PCR was performed using Light Cycler (Roche Diagnostics) technology. When appropriate, products were electrophoresed in 2% agarose gels. All transcript values are shown as mean values ± standard error measurement (SEM) relative to β-actin. Cycling parameters are available upon request. Primer sequences are provided in Supplemental Table 1.

FACS analysis and sorting of hematopoietic cell populations

Upon dissection, the plunger of a 5 mL syringe was used to dissociate thymus and spleen tissues. Cells were strained through a 100 μm filter and collected in 10 mL of FACS buffer (1x PBS + 0.1% BSA). Bone marrow was collected from both femurs and tibias. Removing the ends of each bone with a razor blade exposed bone cavities. Marrow was flushed from cavities using a $25^{5/8}$G syringe and FACS buffer. Contents were collected in 8 mL of FACS buffer. After centrifugation, erythrocytes were lysed on ice for ten minutes using ACK buffer. Following lysis, cells were respun, resuspended in FACS buffer and counted using a Hemoctyometer. Cells were stained on ice for 30 minutes using the appropriate antibody cocktail. Samples were washed with FACS buffer, centrifuged and resuspended in FACS buffer. To discriminate between live and dead cells, DAPI was added at a final concentration of 3 μm. The antibodies utilized with their indicated dilutions are available in Supplemental Table 1. Population analysis was performed on the FACS Canto II (BD Biosciences) and results for a given cell type are graphically represented as mean values ± standard error measurement (SEM) of total live cells or ratios of live cells analyzed per tissue. Cell sorting of select populations was performed on the Aria Cell Sorter (BD Biosciences) at the University of Utah Flow Cytometry Core.

Analysis of whole blood cell populations

Blood was collected in heparinized capillaries via the retro-orbital route. Complete blood counts were obtained using a Hemavet 950 FS (Drew Scientific). Results for a given parameter are listed in Supplemental Table 2 and are represented as mean values ± standard error measurement (SEM).

RNA-Seq Analysis

5×10^5 splenic CD19+ B cells were FACS-sorted from three WT and three *Zfp318* cKO mice. Total RNA was isolated as described in *RNA isolation, cDNA synthesis and RT-PCR.* 50 ng of total RNA was utilized for RNA-Seq library preparation using the Illumina TruSeq RNA Sample Preparation kit with the polyA enrichment step omitted. Libraries were subjected to HiSeq2000 50 Cycle Single Read Sequencing. Greater than 20×10^6 reads per sample were obtained and aligned to the mm10 (Ensembl build 75) transcriptome index using Novoalign. Aligned reads were further processed for splicing and expression variance using the Useq 8.7.4 software package. Data tracks were visualized with the University of California-Santa Cruz genome browser.

Statistical analysis

For FACS, RT-PCR and complete blood count data, two-tailed unpaired Student's t-tests were applied for all relevant statistical comparisons using GraphPad Prism software. For RNA-Seq analysis, two-tailed Student's t-tests using two-sample equal variance were performed using Microsoft Excel. Statistical cutoffs are noted in the figure legends.

Results

Analysis of Zfp318 expression, the generation of a Zfp318 deficient animal and analysis of B cell development in the absence of Zfp318

Our previous screen of maturing and mature B cells for the expression of Zfp318 utilized gene grid array analysis of pooled age- and tissue-specific B cells(6). To expand and specify the time frame of *Zfp318* expression during B cell development, we FACS sorted and isolated Pro, Pre and Newly Formed (NF) B cells from the bone marrow, and T1, T2, MZ and FO B cells from the spleen (Supplemental Fig. 1). RNA was extracted and analyzed for *Zfp318* specific transcripts. As shown in Fig. 1 A, the presence of the *Zfp318* transcript parallels the maturity of the cell, similar to our previous observation. Interestingly while the FO cells showed the highest level of expression the MZ cells had dramatically less *Zfp318* transcript, similar to levels seen in the NF marrow population.

To create a conditional Zfp318 deficient animal, we generated a targeting construct that possessed a LoxP site upstream of the transcriptional start site and a second LoxP site about 7,000 bp 3′ (Fig.1 B). Deletion of the sequences between the two LoxP sites would thus remove the promoter sequences, the initiating ATG and the first two coding exons of the gene. This construct was used to create a germ line targeted animal which was then bred to the *Vav-Cre* deleter line (maintained as a heterozygote). Genotyping of this animal (Fig.1 C) for the WT and flox'd/knockin alleles was done using PCR primers specific for the products and DNA isolated from either the tail or bone marrow of heterozygote (*WT/fl*) or homozygous *Zfp318* targeted animals (*fl/fl*) with or without the *Vav-Cre* deleter transgene. Using the P1 and P2 PCR primers, the 175bp fragment of WT DNA is evident as is the same sequence containing the inserted LoxP site in the tail of the heterozygote and KO. However, that sequence is entirely lost in the marrow of the KO animal possessing the *Vav-Cre* construct indicating a very efficient deletion of those sequences in the tissue expressing the *Vav-Cre* transgene. The loss of *Zfp318* expression was confirmed and quantified in the spleen of the conditional KO animal (cKO) compared to that of WT (Fig.1 D) using the primers described in Supplemental Table 1 (4913/4914).

The development of B cells in the cKO animal was analyzed. The percentage of CD19+ cells and quantification of total cells of the marrow (Fig.2 A) was analyzed using markers to define the Pro, Pre, NF and mature, recirculating B cells (Recirc)(CD22+AA4.1-) in 4wk old animals. There was no significant difference between the WT and cKO marrow samples. A similar analysis was carried out using the T1, T2, MZ and FO populations of the spleen (Fig. 2 B). Again the cKO animals closely tracked with WT animals except for a slight but significant depression in T2 B cells in the cKO animals. Hemavet analysis of peripheral blood also showed no significant difference between WT and the *Zfp318* cKO animal (Supplemental Table 2).

The absence of Zfp318 results in the loss of IgD

The previous analyses indicated that the development of mature B cells in the cKO animal was very similar to that of WT, but did not determine if the lack of Zfp318 altered the expression of B cell gene products. As a primary screen we analyzed the cKO splenic B

cells for the expression of mature marker proteins such as CD35, CD21, B220 and CD19 and found expression levels of these proteins indistinguishable from WT (Fig. 3 A-C). When assaying for the expression of IgM and IgD, the two immunoglobulins expressed by mature naïve B cells, we were surprised to find the level of IgM elevated in the cKO animals compared to WT. As shown in Fig. 3 D, cells from the cKO animal (grey filled plot) expressed significantly higher levels of IgM than either WT or the *Zfp318* cKO heterozygote animal (HET) in the T2 and FO populations. The analysis of IgD expression demonstrated the complete lack of IgD surface protein on cells of T1, T2, MZ and FO populations compared to WT and heterozygote animals (Fig.3 E). The differences in expression levels of IgM and IgD were quantified by analysis of mean fluorescence intensity (MFI) in the WT and cKO populations (Fig. 3 F). The elevated level of expression of IgM in the cKO cells was significantly different from that of WT in the T2, FO and MZ populations while the loss of IgD in the T1, T2, FO and MZ populations was significantly different in the cKO samples.

Both IgM and IgD are encoded from a single heterogeneous nuclear (hnRNA) transcript via alternative splicing of the VDJ sequences to those exons encoding the constant region domains. To determine if these differences in surface expression of IgD and IgM on the surface of *Zfp318* deficient B cells were reflected in transcripts specific for the IgM and IgD products, quantitative RT-PCR was performed using RNA obtained from total spleen (WT and cKO) and analyzed using primers specific for the IgM (*Ighm*) and IgD (*Ighd*) constant regions. As shown in Fig. 3 G, the level of IgM transcripts trended higher in the cKO animal while those encoding IgD in the cKO animal were reduced greater than 90% compared to WT. These data, in total, suggest that the absence of the Zfp318 protein does not alter the *transcriptional activity* of the locus encoding the IgM and IgD proteins, but does alter the relative proportion of transcripts destined to encode the IgM and IgD proteins.

The absence of Zfp318 blocks IgD production by transcriptional termination at the end of the IgM-encoding exons

The loss of IgD-encoding transcripts (and IgD protein) in the absence of Zfp318 suggested this protein alters transcript quantities. To determine if this effect was unique to that of IgD, we performed RNA-Seq using RNA obtained from purified CD19+ splenic B cells from three WT and three cKO animals (Supplemental Table 3). Analysis of those data indicated only three gene products showed significantly altered expression in the cKO animals: the *Zfp318* gene itself, the region of the *Ighm/Ighd* locus encoding the IgD protein and *Sva*, a gene on mouse chromosome 6 that encodes a “seminal vesicle antigen” unique to mice (Fig. 4 A). RNA-Seq data from three genes are shown (Fig. 4 B-D) using one representative WT and cKO sample. As expected *Zfp318* transcripts are absent in the cDKO (Fig. 4 B), the *Cr2* gene products (which produces the Cr1 and Cr2 proteins via alternative splicing) are identical between the two samples (Fig. 4 C), and the *Ighm* and *Ighd* loci show IgM-specific transcripts in both WT and cKO, but the absence of IgD-specific transcripts in the cKO animal (Fig. 4 D). Therefore, in these B cell populations, Zfp318 uniquely influences only *Ighd* and *Sva* expression.

The loss of IgD-encoding transcripts in the cKO B cells could be due to at least two mechanisms: blocking the alternative splicing of the IgM and IgD-encoding transcripts, or blocking the hnRNA transcription of the *Ighm* locus to the sequences encoding the IgD protein. The *Ighm/Ighd* locus contains at least three distinct transcriptional stop sites including one just 3′ of the exons encoding secreted IgM, a second site allowing for the production of membrane bound IgM and a third site 3′ of the last exon encoding the mature, membrane bound IgD protein (16-19). To encode both IgM and IgD via alternative splicing of hnRNA, the transcriptional stop sites linked to the IgM-encoding exons must be ignored by the Pol II RNA polymerase complex. A close analysis of the RNA-Seq data obtained from the *Ighm/Ighd* locus revealed a dramatic loss of virtually all RNA transcripts 3′ of the IgM-encoding exons (Fig. 5 A) suggesting the production of hnRNA containing the IgD-encoding sequences was significantly reduced in the absence of Zfp318.

The production of *Ighm*/*Ighd* hnRNA in the cKO animal was further quantified by RT-PCR analysis of intronic sequences from IgM-encoding and IgD-encoding regions of the locus. Two primer sets (Fig. 5 A) were used to screen total RNA via RT-PCR. The first primer set (Primer Set A) included an IgM-specific intronic sequence and a turnaround within the last exon of the IgM region, while the second set of primers (Primer Set B) was 3′ of the *Ighm* transcriptional stop site to generate membrane-bound IgM. The relative products from these two sets of primers were quantified (Fig. 5 B) by establishing a ratio of the IgD-intronic sequence (Primer Set B) versus the IgM-intronic sequence (Primer Set A). Clearly there is a marked change in ratio of these intronic sequences comparing the WT to the cKO samples (70% reduction in the cKO). RT-PCR analyses of RNA samples can be clouded by the presence of genomic DNA. To control for this, triplicate WT and cKO RNA samples (and genomic DNA as control) were analyzed using primers specific for a region of the *Cd3*ε gene that is not transcribed, and using an oligo set within the final coding exon of the IgM protein (Primer Set C) (Fig. 5 A). The cDNA samples obtained from the WT and cKO RNA samples did not demonstrate amplification of the *Cd3*ε associated sequences but did show equal quantities of the *Ighm* gene product (Fig. 5 B) indicating the amplification of genomic sequences from the IgM- and IgD-encoding regions of the *Ighm* locus was from hnRNA, not genomic DNA.

Discussion

Naïve FO cells express both IgM and IgD, while MZ cells preferentially express IgM (Fig. 6 B,C). Expression of *Ighd* in naïve maturing B cells closely parallels that of *Zfp318* (Fig. 6A,C from Fig. 1 A). Upon activation, FO B cells depress IgD expression and, with additional stimulation and T cell help, class switch to additional antibody isotypes. The historical view of IgM versus IgD production has been based upon an alternative splicing model in which the same VDJ coding sequences are alternatively spliced to exons encoding the constant regions of IgM or IgD. Clearly this requires an hnRNA that encompasses the entire *Ighm/Ighd* locus.

Currently, there is very little known about what regulates the differential expression of transcripts coding for IgM and IgD via alternative splicing of a common VDJ region to the IgM- or IgD-encoding exons. Indeed the best parallel to this system may be in the analysis

of the U1A-mediated regulation of membrane versus secreted IgM. Similar to Zfp318, U1A expression levels are regulated throughout B cell development/differentiation with high expression being required for the repression of secretory IgM(20). U1A acts to block the expression of secretory IgM by impairing the binding and hence, downstream function of the polyA cleavage complex which includes CPSF, Cstf and polyA polymerase (PAP) (20-23). U1A mediates this suppression by interacting with multiple non-consensus U1A-binding sites (AUGC-core) both upstream and downstream of the AAUAAA polyA signal. Due to the nature of these binding sites, a mass action effect of U1A is required to achieve full repression. A similar scenario may be true for the function of Zfp318 as high *Zfp318* gene expression levels correlate with high *Ighd* levels in various B cell populations (Fig 6). Similar to the secretory IgM polyA site, there are three AUGC sites clustered approximately 500 bp upstream of the membrane IgM polyA signal. Whether these binding sites are functional for Zfp318 recognition remains to be determined. However, Zfp318 does possess multiple U1-RNA zinc finger domains thus it is tempting to speculate that Zfp318 regulates *Ighm/Ighd* gene transcription by binding to these AUGC sites. An alternative possibility is that Zfp318 may interact with a yet to be determined binding site(s) and serves to stabilize the binding of U1A leading to a more stable repression of polyA usage. This idea is partially supported by data in Fig 5 showing the 70% loss of transcription downstream of the membrane IgM polyA signal rather than a complete block upon *Zfp318* deletion.

Our analysis of Zfp318 deficient B cells shows that the absence of IgD expression is linked to the preferential usage of a transcriptional stop site located within the final *Ighm* exon, thus blocking the synthesis of the full *Ighm/Ighd* hnRNA which is required for the production of IgD (Fig. 6 D) (16, 18). This finding implicates the Zfp318 protein as functioning to block recognition of the IgM-specific transcriptional stop site allowing for the RNA Pol II complex to proceed down the chromosome into the IgD-encoding region. This finding suggests Zfp318, which possesses two putative nucleic acid binding zinc finger domains (7), recognizes the IgM-specific transcriptional stop site and inhibits transcription termination at that site, possibly by inhibiting RNA pausing and transcription termination via the cleavage and polyadenylation specificity factor (CPSF) protein complexes or those required for cleavage (24-26). It also suggests that the regulation of *Zfp318* is intimately tied to B cell differentiation (MZ B cells express low levels of both *Zfp318* and IgD while FO cells express much higher levels of both gene products) and that FO B cell activation which results in the loss of IgD (but expression of IgM) may also regulate the expression of *Zfp318*.

We know of no other instance in mammalian cells in which a transcription stop site is blocked, in a similar fashion as we see for the *Ighm* locus, to allow for the production of a longer hnRNA molecule and increased genetic capacity. The IgM-encoding region of *Ighm* also possesses a transcription stop site that generates the smaller, secreted form of the protein that must also be ignored by the Pol II complex in the naïve B cell. This site is not blocked by Zfp318, if it was we might have expected only secreted IgM in the absence of Zfp318. However, whether or not this second site is blocked by another protein functioning in an analogous fashion to Zfp318 is not known.

The expression of *Zfp318* parallels that of other transcriptional regulators during the maturation and development of B cells. One such regulator, Mef2c, also demonstrates enhanced expression in FO cells compared to MZ cells. Our previously published analysis of Mef2c-deficient B cells demonstrated a dramatic reduction in expression of *Zfp318* (27). This reduction in *Zfp318* expression, however, was not to the same magnitude as a *Zfp318* gene deficiency. Indeed, B cells lacking Mef2c still express IgD (28) suggesting that sufficient Zfp318 was present to allow for *Ighd* transcription. The analyses of our *Zfp318* deficiency via *Vav-Cre* phenocopies the results described by Enders, et al, although a relative depression of T2 B cells of the spleen was not noted in their report (15). Enders, et al, further suggested that Zfp318 served to regulate IgD production by controlling the alternative splicing of the hnRNA of the *Ighm/Ighd* locus although no data were presented to support this model (15). Our conclusions as to the proposed function of Zfp318 differ from those presented of Enders, et al. due to our RNA-Seq data which point to the regulation of transcription termination as the event which subsequently allows for the production of IgD via alternative splicing. Thus it is the primary production of the *Ighm/Ighd* hnRNA which is the key step regulated by Zfp318, not the alternative splicing choice of the VDJ sequence to either the IgM- or IgD-encoding exons.

Supplementary Material

Refer to Web version on PubMed Central for supplementary material.

Acknowledgments

The authors would like to thank the University of Utah Core facilities (FACS, RNA-Seq, Transgenic and Knockout Mouse and Data Analysis) and specifically Dr's. Susan Tomowski, David Nix and Tim Mosbruger for assistance, and Dr. Dean Tantin for the use of his Hemavet. We would like to thank the members of the Weis labs for their critique of this work and many useful suggestions.

References

1. Su TT, Rawlings DJ. Transitional B lymphocyte subsets operate as distinct checkpoints in murine splenic B cell development. J Immunol. 2002; 168:2101–2110. [PubMed: 11859095]
2. Busslinger M. Transcriptional control of early B cell development. Annu Rev Immunol. 2004; 22:55–79. [PubMed: 15032574]
3. Mandel EM, Grosschedl R. Transcription control of early B cell differentiation. Curr Opin Immunol. 2010; 22:161–167. [PubMed: 20144854]
4. Matthias P, Rolink AG. Transcriptional networks in developing and mature B cells. Nat Rev Immunol. 2005; 5:497–508. [PubMed: 15928681]
5. Hardy RR, Kincade PW, Dorshkind K. The protean nature of cells in the B lymphocyte lineage. Immunity. 2007; 26:703–714. [PubMed: 17582343]
6. Debnath I, Roundy KM, Dunn DM, Weiss RB, Weis JJ, Weis JH. Defining a transcriptional fingerprint of murine splenic B-cell development. Genes Immun. 2008; 9:706–720. [PubMed: 18784731]
7. Ishizuka M, Ohshima H, Tamura N, Nakada T, Inoue A, Hirose S, Hagiwara H. Molecular cloning and characteristics of a novel zinc finger protein and its splice variant whose transcripts are expressed during spermatogenesis. Biochem Biophys Res Commun. 2003; 301:1079–1085. [PubMed: 12589823]
8. Inoue A, Ishiji A, Kasagi S, Ishizuka M, Hirose S, Baba T, Hagiwara H. The transcript for a novel protein with a zinc finger motif is expressed at specific stages of mouse spermatogenesis. Biochem Biophys Res Commun. 2000; 273:398–403. [PubMed: 10873617]

9. Tao RH, Kawate H, Ohnaka K, Ishizuka M, Hagiwara H, Takayanagi R. Opposite effects of alternative TZF spliced variants on androgen receptor. Biochem Biophys Res Commun. 2006; 341:515–521. [PubMed: 16446156]
10. Wilson CA, Mrose SA, Thomas DW. Enhanced production of B lymphocytes after castration. Blood. 1995; 85:1535–1539. [PubMed: 7534134]
11. Erben RG, Eberle J, Stangassinger M. B lymphopoiesis is upregulated after orchiectomy and is correlated with estradiol but not testosterone serum levels in aged male rats. Horm Metab Res. 2001; 33:491–498. [PubMed: 11544564]
12. Altuwaijri S, Chuang KH, Lai KP, Lai JJ, Lin HY, Young FM, Bottaro A, Tsai MY, Zeng WP, Chang HC, Yeh S, Chang C. Susceptibility to autoimmunity and B cell resistance to apoptosis in mice lacking androgen receptor in B cells. Mol Endocrinol. 2009; 23:444–453. [PubMed: 19164450]
13. Treiber T, Mandel EM, Pott S, Gyory I, Firner S, Liu ET, Grosschedl R. Early B cell factor 1 regulates B cell gene networks by activation, repression, and transcription-independent poising of chromatin. Immunity. 2010; 32:714–725. [PubMed: 20451411]
14. Yuan D,P, Witte L, Tan J, Hawley J, Dang T. Regulation of IgM and IgD heavy chain gene expression: effect of abrogation of intergenic transcriptional termination. J Immunol. 1996; 157:2073–2081. [PubMed: 8757329]
15. Enders A, Short A, Miosge LA, Bergmann H, Sontani Y, Bertram EM, Whittle B, Balakishnan B, Yoshida K, Sjollema G, Field MA, Andrews TD, Hagiwara H, Goodnow CC. Zinc-finger protein ZFP318 is essential for expression of IgD, the alternatively spliced Igh product made by mature B lymphocytes. Proc Natl Acad Sci U S A. 2014; 111:4513–4518. [PubMed: 24616512]
16. Danner D, Leder P. Role of an RNA cleavage/poly(A) addition site in the production of membrane-bound and secreted IgM mRNA. Proc Natl Acad Sci U S A. 1985; 82:8658–8662. [PubMed: 3936040]
17. Early P, Rogers J, Davis M, Calame K, Bond M, Wall R, Hood L. Two mRNAs can be produced from a single immunoglobulin mu gene by alternative RNA processing pathways. Cell. 1980; 20:313–319. [PubMed: 6771020]
18. Rogers J, Early P, Carter C, Calame K, Bond M, Hood L, Wall R. Two mRNAs with different 3′ ends encode membrane-bound and secreted forms of immunoglobulin mu chain. Cell. 1980; 20:303–312. [PubMed: 6771019]
19. Alt FW, Bothwell AL, Knapp M, Siden E, Mather E, Koshland M, Baltimore D. Synthesis of secreted and membrane-bound immunoglobulin mu heavy chains is directed by mRNAs that differ at their 3′ ends. Cell. 1980; 20:293–301. [PubMed: 6771018]
20. Ma J, Gunderson SI, Phillips C. Non-snRNP U1A levels decrease during mammalian B-cell differentiation and release the IgM secretory poly(A) site from repression. Rna. 2006; 12:122–132. [PubMed: 16373497]
21. Phillips C, Pachikara N, Gunderson SI. U1A inhibits cleavage at the immunoglobulin M heavy-chain secretory poly(A) site by binding between the two downstream GU-rich regions. Mol Cell Biol. 2004; 24:6162–6171. [PubMed: 15226420]
22. Phillips C, Gunderson S. Sequences adjacent to the 5′ splice site control U1A binding upstream of the IgM heavy chain secretory poly(A) site. J Biol Chem. 2003; 278:22102–22111. [PubMed: 12670951]
23. Phillips C, Jung S, Gunderson SI. Regulation of nuclear poly(A) addition controls the expression of immunoglobulin M secretory mRNA. Embo J. 2001; 20:6443–6452. [PubMed: 11707415]
24. Richard P, Manley JL. Transcription termination by nuclear RNA polymerases. Genes Dev. 2009; 23:1247–1269. [PubMed: 19487567]
25. Glover-Cutter K, Kim S, Espinosa J, Bentley DL. RNA polymerase II pauses and associates with pre-mRNA processing factors at both ends of genes. Nat Struct Mol Biol. 2008; 15:71–78. [PubMed: 18157150]
26. Nag A, Narsinh K, Martinson HG. The poly(A)-dependent transcriptional pause is mediated by CPSF acting on the body of the polymerase. Nat Struct Mol Biol. 2007; 14:662–669. [PubMed: 17572685]

27. Debnath I, Roundy KM, Pioli PD, Weis JJ, Weis JH. Bone marrow-induced Mef2c deficiency delays B-cell development and alters the expression of key B-cell regulatory proteins. Int Immunol. 2013; 25:99–115. [PubMed: 23087187]

28. Khiem D, Cyster JG, Schwarz JJ, Black BL. A p38 MAPK-MEF2C pathway regulates B-cell proliferation. Proc Natl Acad Sci U S A. 2008; 105:17067–17072. [PubMed: 18955699]

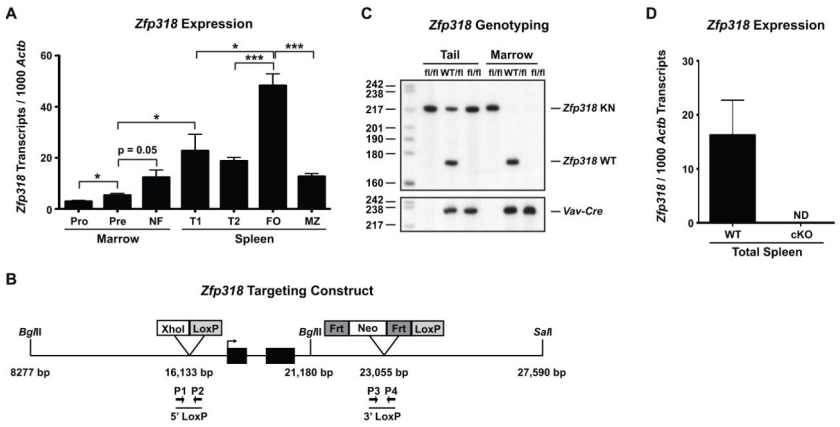

Figure 1. *Zfp318* is highly expressed in mature follicular B cells and is conditionally deleted via *Vav-Cre*

(A) RT-PCR of cDNA derived from the indicated B cell subsets. Four biological replicates were assayed for each subset. NF = Newly Formed, T1 = Transitional 1, T2 = Transitional 2, FO = Follicular, MZ = Marginal Zone; Statistics: * $p < 0.05$, ** $p < 0.01$, *** $p < 0.001$ (B) Schematic diagram of the $Zfp318^{Fl/Fl}$ conditional allele. Cre-mediated recombination of *LoxP* sites results in the deletion of the *Zfp318* proximal promoter as well as exons 1 and 2 (black boxes). (C) Representative genotyping of animals possessing targeted alleles (*fl/fl*) or heterozygous alleles (*WT/fl*) in the presence or absence of the *Vav-Cre* deleter construct. Analysis of genomic DNA isolated from the tail or bone marrow shown using primer set P1/P2 (Supplemental Table 1). The $Zfp318^{fl/fl}$ (*Zfp318* KN) allele is only deleted in cells isolated from the bone marrow demonstrating the hematopoietic specificity of gene deletion. (D) Loss of *Zfp318* transcripts was validated using cDNA derived from WT and cKO total spleen tissues. Three biological replicates were performed per genotype. ND = Not Detected; For (A) and (D), *Zfp318* transcripts were normalized to *Actb* and data is represented as the mean ± SEM.

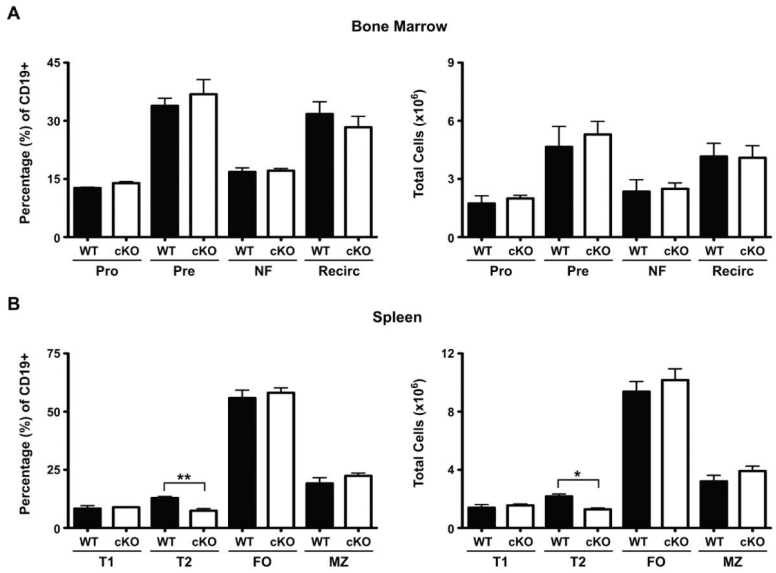

Figure 2. FACS analysis of B cell development in the *Zfp318* conditional knockout animal

(A) Bone marrow and (B) spleen tissues from WT and cDKO animals were assessed by FACS for the disruption of B cell development as a result of *Zfp318* deletion. Three to four animals per group were analyzed. In panels (A) and (B), data represents mean percentage (Left) or absolute cell count (Right) ± SEM for an indicated cell population. NF = Newly Formed, Recirc = Mature Recirculating, T1 = Transitional 1, T2 = Transitional 2, FO = Follicular, MZ = Marginal Zone; Statistics: * $p < 0.05$, ** $p < 0.01$

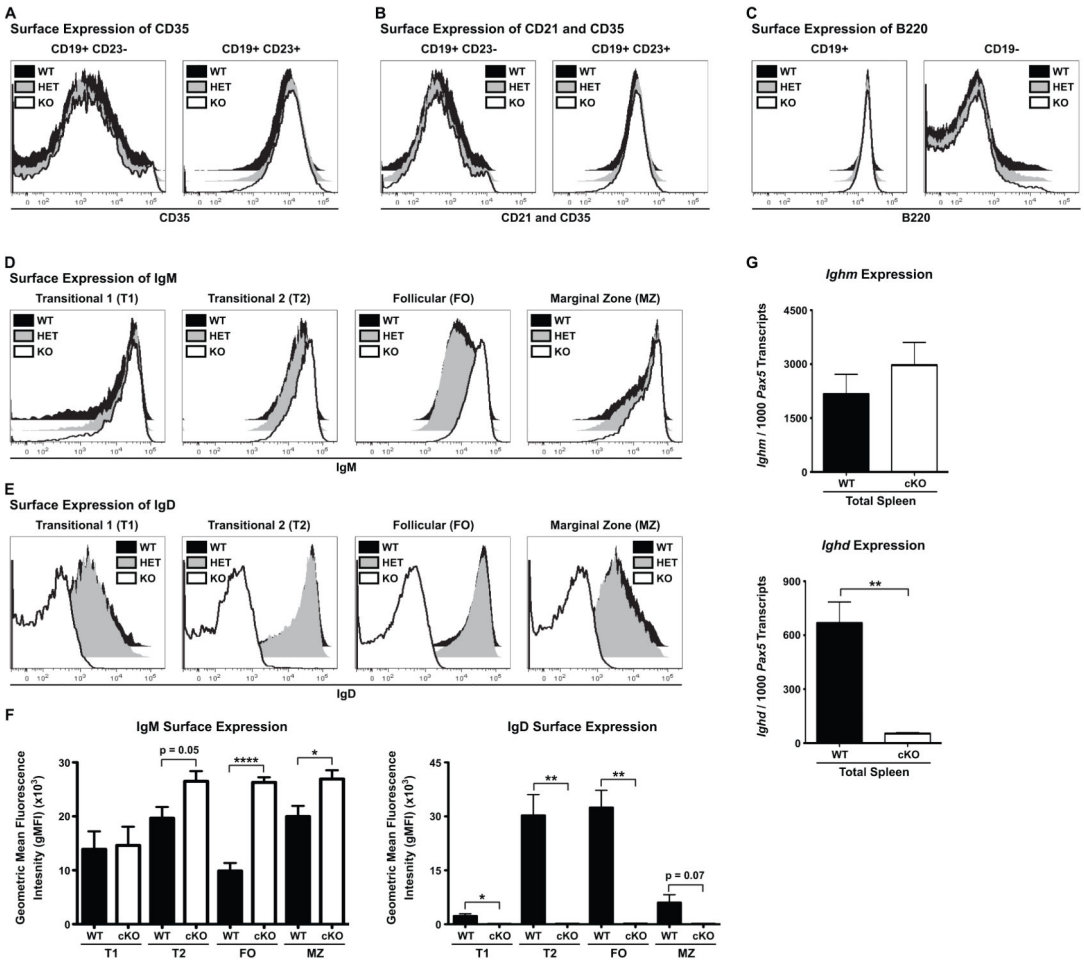

Figure 3. Deletion of *Zfp318* abrogates surface expression of IgD on B cells

(A-C) Representative mean fluorescence intensity histograms for WT, heterozygous (HET) and knockout (cKO) animals. (A) CD35 and (B) CD21 and CD35 are equally expressed on the surface of splenic CD19+ CD23+/− B cells from all genotypes. (C) B220 is properly expressed by splenic CD19+ B cells and is still repressed by CD19-non-B cell spleen populations. (D-E) Representative mean fluorescence intensity histograms for WT, heterozygous (HET) and knockout (cKO) splenic B cell populations. Upon deletion of *Zfp318*, (D) IgM surface expression is upregulated and (E) IgD surface expression is abrogated. (F) Quantification of geometric mean fluorescence intensities of B cell populations analyzed in (D) and (E). (G) RT-PCR analysis of total spleen cDNA from WT and cKO animals. Three animals per genotype were analyzed. *Ighm* (top panel) and *Ighd* (bottom panel) transcripts were normalized to *Pax5* to compensate for any variance in total B cell contribution. Expression of *Ighd* was reduced >90% in the cKO spleen. Statistics for (F) and (G): * $p < 0.05$, ** $p < 0.01$, **** $p < 0.0001$

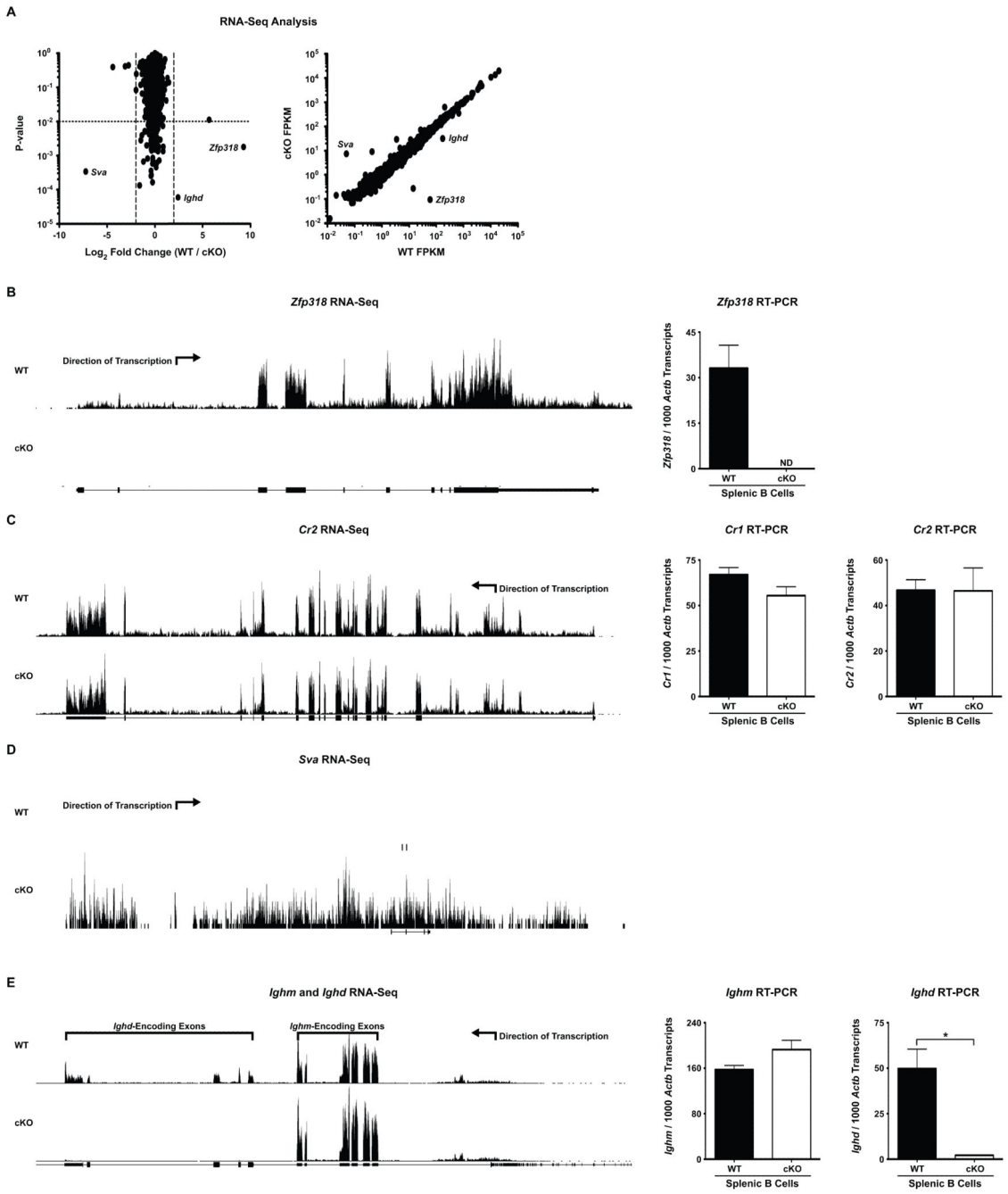

Figure 4. RNA-Seq analysis of CD19+ splenic B cells from WT and *Zfp318* deficient animals

(A) Transcriptome analysis of WT and cKO splenic CD19+ B cells. Three replicates per genotype were sequenced and analyzed (Supplemental Table 3). On the left, Log_2 Fold Change per gene between WT and cKO samples is plotted against the P-value. On the right, WT and cKO FPKM are plotted for all genes analyzed. Genes were considered significantly altered with a Log_2 Fold Change >2 and a P-value < 0.01. (B-D) Representative custom tracks (Left) and RT-PCR validation (Right) for selected genes of interest. (B) *Zfp318* expression is lost in the knockout samples. (C) The alternatively spliced *Cr2* locus

demonstrates equivalent expression in WT and cKO CD19+ B cells. (D) Expression of the *Ighm/Ighd* locus is significantly impaired in the cKO specific to the regions for the IgD-encoding exons (*Ighd*) (>95% reduction). Statistics: * $p < 0.05$

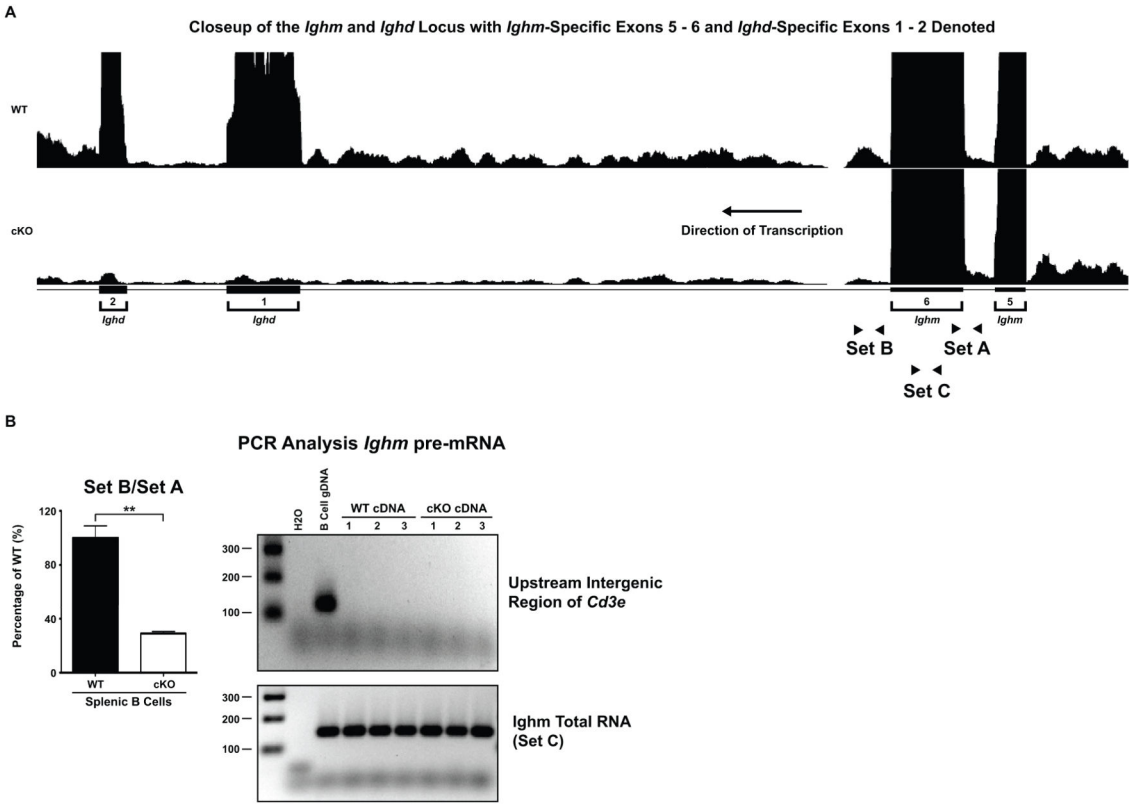

Figure 5. Deletion of *Zfp318* blocks transcription downstream of the terminal *Ighm*-specific exon

(A) Representative RNA-Seq custom tracks from WT and cKO CD19+ B cells illustrating *Ighm*-specific exons 5-6, the intervening intronic region and *Ighd*-specific exons 1-2. Primer sets used to quantify transcription throughout the *Ighm* locus are indicated. (B) LightCycler-based RT-PCR quantification of transcription downstream of *Ighm*-specific exon 6. (Left) For each sample, Ct-derived transcript ratios of SetB/SetA were generated. The mean WT value was used to derive the "percentage of WT" for each individual sample (e.g. WT-1/WT-mean or cKO-1/WT-mean). Statistics: ** $p < 0.01$ (Right) Amplification products from a *Cd3ε* upstream non-coding intergenic region (Top) and from a region internal to IgM-specific exon 6 (Set C) (Bottom).

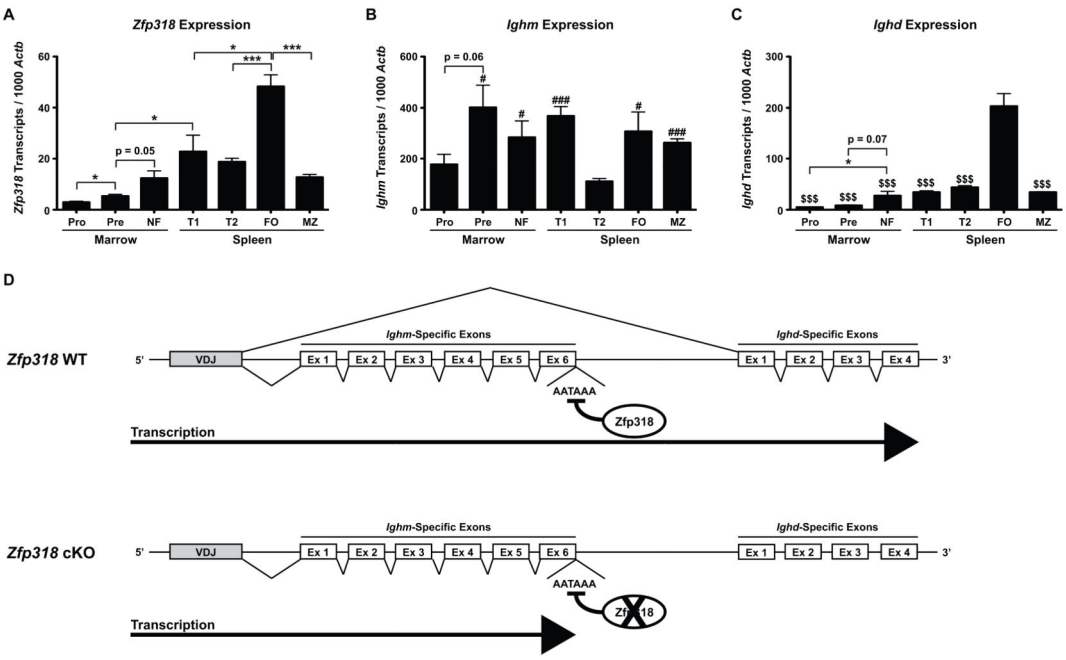

Figure 6. Model of Zfp318 transcriptional regulation throughout the *Ighm* locus

(A-C) Quantification of (A) *Zfp318*, (B) *Ighm* and (C) *Ighd* coding transcripts within the indicated B cell subsets. Panel A was reproduced from Fig. 1A. NF = Newly Formed, T1 = Transitional 1, T2 = Transitional 2, FO = Follicular, MZ = Marginal Zone; Statistics: * $p < 0.05$, ** $p < 0.01$, *** $p < 0.001$ In (B), # represents comparisons between the indicated cell type and the T2 population with # $p < 0.05$ and ### $p < 0.001$. In (C), $ represents comparisons between the indicated cell type and the FO population with $$$ $p < 0.001$. (D) Stylized depiction of transcription throughout the *Ighm/Ighd* locus (not drawn to scale). In the presence of Zfp318 (Top), transcriptional termination is blocked and transcription continues past the terminal *Ighm*-specific exon. This allows for splicing to *Ighd*-specific exons and generation of a mature IgD protein. Upon the loss of Zfp318 (Bottom), transcription is terminated at the final *Ighm*-specific exon. As a result, the downstream *Ighd*-specific exons cannot be transcribed or spliced into a mature transcript.